



On the effects of leakages in Sliding Rotary Vane Expanders

Fabio Fatigati^{*}, Marco Di Bartolomeo, Roberto Cipollone

University of L'Aquila, Department of Industrial and Information Engineering and Economics, Via Giovanni Gronchi n.18, L'Aquila, Italy



ARTICLE INFO

Article history:

Received 26 December 2018

Received in revised form

28 September 2019

Accepted 6 December 2019

Available online 7 December 2019

Keywords:

Dual-intake expanders

ICE bottoming ORC

Waste heat recovery

Volumetric losses

Volumetric expanders

ABSTRACT

Rotary Vane Expanders (RVE) are very suitable prime movers for ORC-based power units in on-the-road transportation sector. RVEs suffer volumetric efficiency deficits due to leakages which limit the overall expander efficiency and can vanish their intrinsic benefits with respect to the other prime movers. Making reference to a 2 kW Sliding RVE type (SRVE), the paper presents a theoretical and experimental contribution which goes deep into the effect of leakages inside the machine and aims to quantify their amount and effects on the expander performances. The results showed that the volumetric losses increase the mass flow rate aspirated by the machine if the intake pressure is kept constant. This increase favors a greater recovery from the hot source (up to 50%) but part of it bypasses the vanes, producing a volumetric loss. An interesting feature is that part of this additional mass is exchanged among vanes and this produces a beneficial effect on the indicated power (16.6% increase with respect to the ideal case). The resulting knowledge further supported the effectiveness of dual intake expander technology which allows to theoretically reduce the leakages between adjacent vane up to 60–70% ensuring an improvement of expander efficiency.

© 2019 Elsevier Ltd. All rights reserved.

1. Introduction

The ORC-based technology for Waste Heat Recovery of Internal Combustion Engine (ICE) exhaust gases, differently to stationary fixed applications, has to deal with several critical issues represented by constraints related to some specific aspects for a conversion on board, the management of transient conditions [1,2], and the adopted expander technology. Volumetric expander (alternative or rotary) are the most promising solution for small/medium scale ORC recovery unit [3] due to their higher flexibility and robustness in off-design operating conditions and lower revolution speed with respect axial and radial turbine, [4]. Nevertheless, technical complexities, lubrication requirements, frictional and leakages losses represent the main limiting aspect for the commercialization of volumetric devices. In particular, internal leakages severely affect the efficiency of all volumetric devices and the scientific literature deeply treated this aspect. In scroll machines, the presence of leakages [5] makes the difference between ideal and real behavior in terms of overall expander efficiency [6]. Similarly, for piston expanders the leakages of working fluid between piston and cylinder represent one of the efficiency limiting

aspect and its prediction and addressing are challenging, [7]. Volumetric losses affect also the performances of single screw expanders [8] and clearance height influences also the friction power consumption [9].

Compared with other expanders, Sliding Rotary Vane Expander (SRVE) presents a simpler structure [10,11], lower cost and easier manufacturing. Their overall efficiency doesn't change significantly in a wide range of operating conditions, [12]. SVREs allow also to handle high pressures [13], ensure to reach high volumetric expansion ratios, low noise and vibration's level and easy self-starting, [14]. Nevertheless, they may suffer more leakages with respect to other volumetric machines [15], being the correspondent loss higher than those due to friction, [16]. Thus, a common operating aspect of RVE is the need to mix, inside the expanding fluid, some lubricating oil which reduces leakages and friction, but it produces expansion losses, affects the distribution of working fluid charge in the system [17] and lead to a heat transfer reduction in heat exchanger, [18].

The major part of the leakages inside vane expanders happens between the blade and the stator due to their insufficient contact especially during the charging process of the vanes, [19,20]. Indeed, SVREs can be affected by "blade chatter" [19] which implies that the vanes are not in permanent contact with the stator inner surface, increasing flow leakages between adjacent chambers with the oil thickness unable to ensure vane tip sealing. As demonstrated in

^{*} Corresponding author.

E-mail address: fabio.fatigati@univaq.it (F. Fatigati).

Nomenclature	
A	Area [m ²]
C	Coefficient
D	Equivalent diameter [mm]
dp	Pressure difference [MPa]
dx	Discretization length [mm]
e	Specific internal total energy [kJ/kg]
F	Force [N]
H	Specific total enthalpy [kJ/kg]
h	Specific Enthalpy [kJ/kg]
L	Length [m]
m	Mass [kg]
\dot{m}	Mass flow rate [kg/s]
N_v	Vane Number
OEM	Original Equipment Manufacturing
p	Pressure [MPa]
R_{blade}	Actual blade radius [mm]
t	Time [s]
T	Temperature [K]
u	Working fluid velocity [m/s]
V	Volume [m ³]
V	Vane
x	Vapor quality
<i>Subscript</i>	
blade	Blade
blade,tip	Blade tip
dual int	Dual intake port
end	Port closing
in	Inlet
dual int	Dual intake port
exh	Exhaust port
exp	Expander global efficiency
flow	Cross sectional area
i	Generic i-vane
int	Intake port
leak	Leak flow
out	Outlet
p	Pressure drop coefficient
SH	Super heating
start	Port opening
wall	Wall temperature
WF	Working Fluid
<i>Greek symbol</i>	
Δp	Pressure difference [MPa]
$\Delta\theta$	Angular extent [deg]
$\Phi_{dual\ int}$	Dual intake port position [deg]
η	Efficiency
λ	Convective heat exchange coefficient [W/m ² K]
ρ	Density [kg/m ³]
μ	Dynamic viscosity [Pa s]
ω	Revolution speed [rpm],[rad/s]

Ref. [21] through an experimentally calibrated 1D model, the case in which the blades are not in contact with stator surface in the sealing arc produces the highest impact on expander performance. The results showed as decreasing the expander clearance from 0.150 mm to 0.05 mm the vane expander isentropic efficiency grown from 0.45 to 0.55 while the produced mechanical power from 2.64 to 3.29 kW.

Yang et al. [22] demonstrated that the main cause of the loss of contact is produced by the impact of the inlet gas flow on the vane itself during filling. In order to reduce this clearance gap, solution as spring-loaded blades which ensures to enhance the reaction force at blade tip can be implemented, [22]. In Ref. [23] an alternative solution to reduce the volumetric losses was reported. It consists in the introduction of high pressure working fluid into the vane slots in order to sustain the blades preventing the loss of contact. The adoption of this solution provides an increase of volumetric efficiency from 17 to 35% and of isentropic efficiency from 15 to 45%. Volumetric and friction losses, in reality, can be partially reduced also designing the blade tip in a way which favor the pressurization of the oil film, thus preventing any contact with the inner stator surfaces [24,25]. Nevertheless, when machine works as expander the high pressure level inside the intake vane as well as the high kinetic energy of the fluid jet entering the machine tends to scrape oil thickness and amplify leakages.

Leakages move inside the machine following the negative pressure gradients: this happens across vanes at the tip blades, at the bottom of the slots and across stator lateral side covers. The evidence of the leakage is demonstrated by the difference between the fluid flow rate measured upstream the expander and the one actually introduced inside the vane, [26]. Indeed, as demonstrated by the authors in Ref. [27], the leakages increase the expander permeability defined as the ratio between mass flow rate at expander inlet and the upstream pressure itself. It was experimentally and theoretically demonstrated that keeping constant the

intake pressure, SVREs affected by low volumetric efficiency elaborated a higher mass flow rate with respect to machines with lower volumetric losses. A considerable amount of this extra mass flow rate by-passes the vane representing a severe loss but [28], a significant part moves across adjacent vanes, increasing the pressure inside them. The effects of leakages between adjacent vane on indicated p-V cycle was observed also in Ref. [29] where p-V measurement with fast response pressure transducers shows that real curve (in presence of leakages) is quite different from the p-V data predicted assuming no leakages and an adiabatic isentropic transformation. As observed in Ref. [26], leakages involve also an "artificial" delayed closure of the vane, reducing the pressure decrease during the start of expansion phase when the vanes already passed the intake ports. Thus, although leakages worsen the filling of the suction vane they allow to reduce the pressure decrease of the adjacent vanes which are expanding increasing the indicated power. This provides a recovery effects which partially compensates the leakages detrimental effects on expander efficiency.

A quantitative analysis of the effects on the pressure inside the vanes due to the leakages flow and the partial recovery in terms of indicated power associated were not fully investigated in literature. Moreover, an accurate prediction of internal leakage losses is still an open issues to ensure nominal operation of the expander in real working condition, [30]. In order to put in evidence and quantify these leakages features, in this paper a theoretical and experimental activity was carried out and an explanation of what happens inside the machine caused by the leakages was discerned. Furthermore, the paper aims to outline a novel technology which allow to reduce the leakages impact on expander performance without reducing the mechanical efficiency as it happen with the solutions currently adopted in literature. To reach this goal, the effect of the leakages on expander performance has been discerned thanks to a comprehensive numerical model of the expander

developed in GT-Suite™ environment. The model was validated through an extensive experimental activity done on a 2 kW SVRE operating in an ORC-based power unit using R236fa as working fluid, whose hot thermal source was the exhaust gas of a 3 L IVECO F1C turbocharged diesel engine. The peculiarity of the experimental activity is the measurement of the expander indicated cycle which allows to evaluate the effects of leakages on the p-V cycle and on the volumetric and mechanical efficiency. In fact, the knowledge of p-V cycles allows to correlate the different flow streams between consecutive vanes with the pressure difference among them assessing in this way the cause of the leakages and their recovery effect on indicated power. This novel analysis was used also to explain, from a point of view internal to expander, the increase in the expander's permeability observed by the authors in a previous work [27]. Finally, the benefits introduced in SVRE volumetric efficiency by dual intake port technology (originally conceived only to enhance the machine operating flexibility [31,32]) was evaluated through the analysis of the pressure difference and the fluid flows, whose the in-time-integral represents the mass exchanged between consecutive vanes. This internal fluid-dynamic analysis of leakages flows was not faced in authors previous work [31,32] and represents a further contribution in the characterization of this novel technology.

2. Experimental test bench

The high thermal source of the tested ORC-based power unit is the exhaust gases of a 3 L supercharged diesel engine for light duty application while the low thermal source is represented by tap water. R236fa was selected as working fluid mixed with a POE ISO VG 68 lubricating oil whose amount is 5% of the refrigerant mass in order to reduce the volumetric losses within the expander. R236fa has been chosen for the sake of continuity with previous experimental campaigns [31,32] and its similar thermo-physical properties and lower cost with respect to R245fa which is one of the most suitable working medium in engine waste heat recovery applications [33]. In Fig. 1 and in Table 1 the p-h diagram of R236fa and the main properties are showed. The working fluid selection affects the

Table 1
Main thermodynamic properties of R236fa.

Critical Temperature T_c	398.1 K
Critical Pressure p_c	3.20 MPa
Critical Density ρ_c	551.3 kg/m ³
Saturation Temperature at 0.1 MPa	271.8 K
Saturation Pressure at 373.15 K	1.94 MPa

size and the weight of the ORC-based power unit [34] which can be critical aspects for the ORC integration of the recovery unit in the light-duty vehicle segment, [35]. The working fluid selection can maximize the pressure difference across the expander [13], improving the useful work and thermal energy recovered.

The ORC-based plant is composed by the following components:

- A gear pump driven by an electric motor which pressurizes and provides the working fluid;
- A sliding rotary vane expander SVRE drives an asynchronous 4 poles electric generator. Being the electric machine on the grid, 1500 RPM was the nominal revolution speed. In Table 2 the geometry of the SVRE was reported. The expander is characterized by a radial intake port and two axial discharge ports. Concerning the angular reference, it is important to notice that for the adopted convention, the reference angular position considers the bisecting line of the vane instead of the one of the blades (Fig. 2), thus the angles are shifted of half vane angular extent [31].
- A plate and fin evaporator prototype specially designed to reduce the back pressure exerted on the exhaust of the ICE;
- A plate heat exchanger as condenser cooled by tap water;
- A plenum with a volume of 3 L at the pump intake which ensures a stable flow rate inside the pump and a faster transient reaction.

In order to represent the indicated diagram and deeply analyze the performance of the expander, three high frequency piezo-resistive sensors have been faced to the machine chambers to evaluate the pressure inside vane as a function of rotation angle and vane volume and time. The raw experimental data was refined through a proper post-process algorithm developed to reconstruct the global indicated cycle, [31]. In Table 3 more details of the adopted instruments and the their uncertainties are reported.

3. Numerical model

In order to deeply analyze the role of leakages on expander performance, the numerical model developed by the author in previous works [30,31] has been improved through the comparison with the collected experimental data, in particular comparing the predicted indicated cycle with the measured one. The numerical

Table 2
Sliding Rotary Vane Expander geometry.

Number of Chambers	7
Stator Inner Diameter	75.9 mm
Rotor Outer Diameter	65.0 mm
Eccentricity	5.45 mm
Chamber Width	60.0 mm
Blade length	17 mm
Blade thickness	3.96 mm
Angular vane extent $\Delta\theta_{vane}$	51.4°
Intake port opening angle $\theta_{int,start}$	4.4°
Intake port closing angle $\theta_{int,end}$	48°
Exhaust port opening angle $\theta_{exh,start}$	180°
Exhaust port closing angle $\theta_{exh,end}$	320°

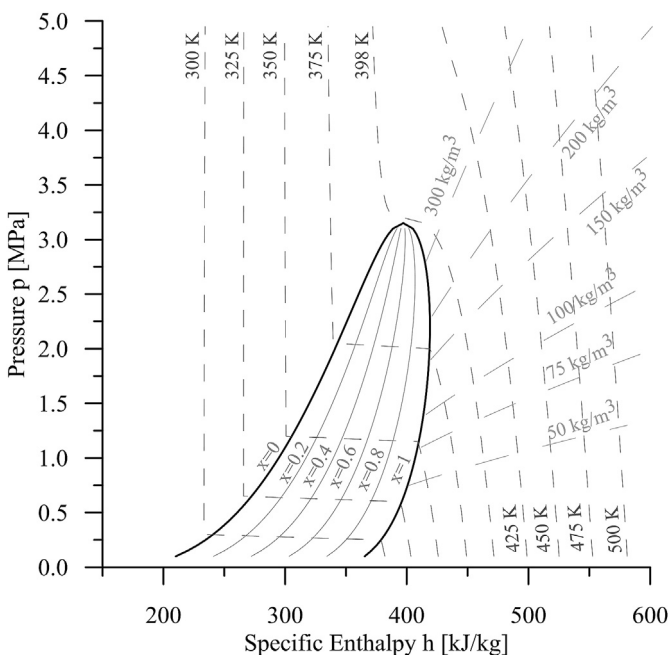


Fig. 1. R236fa p-h diagram where x represents the vapor quality.

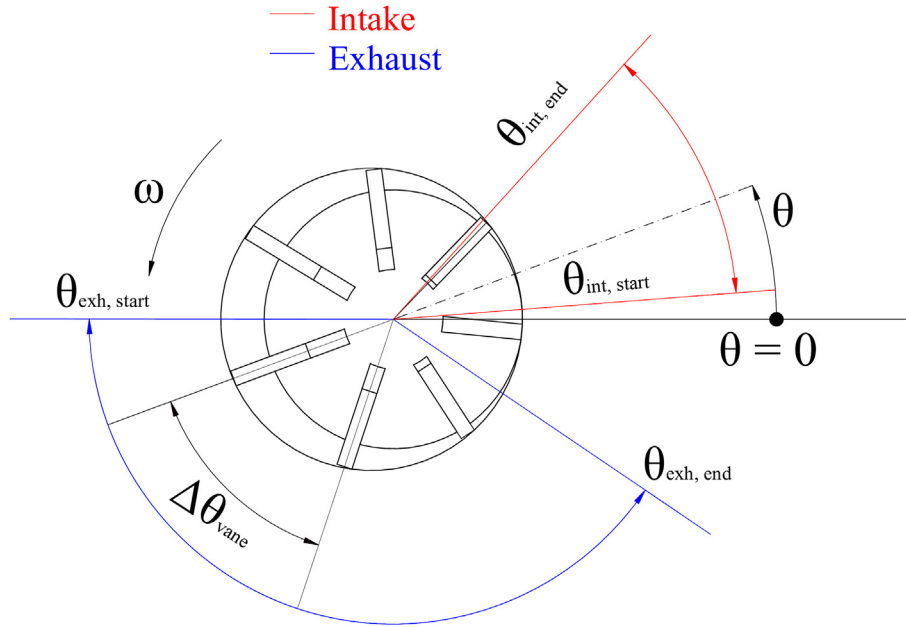


Fig. 2. Sliding vane expander angular reference.

Table 3
Sensor types and uncertainties.

Sensor Type	Measured quantities	Uncertainty
Torque meter	Torque revolution speed	± 0.02 Nm ± 1 RPM
Coriolis Flow Meter	Working fluid mass flow rate Working fluid density Working fluid temperature of working fluid	$\pm 0.5\%$ of measured value ± 20 kg/m ³ ± 0.5 K
Magnetic Flow Meter	Water mass flow rate	$\pm 0.5\%$ of measured value
T-type thermocouple	Working fluid temperature	± 0.3 K
K-type thermocouple	Exhaust gases temperature	± 0.38 K
Static pressure sensor	Working fluid pressure	± 0.03 MPa
Piezo-resistive sensor	Indicated cycle	$\pm 0.1\%$ of the Full Scale Sensor Output

model was developed in GT-Suite™ environment. A mono-dimensional (1-D) analysis was done to predict the dynamic of the fluid inside intake and exhaust pipes, which were discretized into multiple sub-volumes along the characteristic dimension considering all the involved physical quantities uniform on the cross-sectional area, [36]. In each sub-volume, the Navier-Stokes equations which express the conservation of mass (Eq. (1.1)), momentum (Eq. (1.2)) and energy (Eq. (1.3)) are solved to assess the dynamic behavior of the fluid.

$$\frac{dm}{dt} = \sum_{boundaries} \dot{m} \quad (1.1)$$

$$\frac{d\dot{m}}{dt} = \frac{dpA_{flow} + \sum_{boundaries} (\dot{m}u) - 4C_f \frac{\rho u |u| dx A}{2D} - C_p \left(\frac{1}{2} \rho u |u| \right) A}{dx} \quad (1.2)$$

$$\frac{d(me)}{dt} = -p \frac{dV}{dt} + \sum_{boundaries} (\dot{m}H) - \lambda A_s (T_{fluid} - T_{wall}) \quad (1.3)$$

A zero-dimensional (0-D) thermo-fluid-dynamic approach is adopted to model the vanes filling and emptying and the leakages which are calculated by defining a free gap at the tip blade, at the

side covers and between blade side and rotor slot. An extensive theoretical analysis demonstrated that the first contribution is much higher than the others: so, the remaining two terms have been neglected. Once the gap is known, the leakage flow rate is calculated according to the Poiseuille-Couette flow hypothesis [37], as in Eq. (2):

$$Q = A_{blade,tip} \left(\frac{\delta^2 \Delta p}{12\mu L_{leak}} + \frac{1}{2} u_{blade,tip} \right) \quad (2)$$

The model allows also to evaluate the mechanical power lost $P_{mech,lost}$ due to dry and viscous friction effects associated to all the surfaces in relative motion. For the sake of brevity, only the predominant contribute, given by the dry contact between the blade tip and the stator inner surface, is reported (Eq. (3)).

$$P_{mech,lost} = N_v C_f F_n R_{blade} \omega \quad (3)$$

F_n represents the normal force and can be evaluated as the sum of the force explained at the blade bottoming $F_{blade,b}$ by the fluid and the centrifugal force F_c as reported in Eq. (4):

$$F_n = F_{blade,b} + F_c = pA_{blade,b} + m_{blade} \omega^2 \left(R_{blade} - \frac{L_{blade}}{2} \right) \quad (4)$$

Where $A_{blade,b}$ is the blade bottom area. Subtracting the power

lost due to friction phenomena from indicated power, the mechanical power produced P_{mech} by the expander can be evaluated as in Eq. (5):

$$P_{mech} = P_{ind} - P_{mech,lost} \quad (5)$$

The indicated power P_{ind} , is expressed as in Eq. (6):

$$P_{ind} = \frac{\oint \sum_{i=1}^{N_v} p_i dV_i}{t_{cycle}} \quad (6)$$

Therefore, the model is able to assess the volumetric η_{vol} and mechanical η_{mech} efficiency and to produce a comparison with the experimental results. The volumetric efficiency η_{vol} was evaluated as the ratio between the mass flow rate actually aspirated by the vane and that at the expander inlet (Eq. (7)):

$$\eta_{vol} = \frac{\dot{m}_{int}}{\dot{m}_{WF}} = \frac{\dot{m}_{WF} - \dot{m}_{leak}}{\dot{m}_{WF}} \quad (7)$$

So, the difference between \dot{m}_{WF} and \dot{m}_{in} is given by the volumetric losses due to the sum of leakages \dot{m}_{leaks} evaluated by the model. Concerning the mechanical efficiency η_{mech} , it was evaluated as the ratio between the mechanical and the indicated power (Eq. (8)):

$$\eta_{mech} = \frac{P_{mech}}{P_{ind}} \quad (8)$$

Finally, the overall expander efficiency η_{exp} was given by Eq. (9) as the ratio between mechanical power and the one produced by the expander according to an ideal behavior:

$$\eta_{exp} = \frac{P_{mech}}{\dot{m}_{WF}(h_{in} - h_{out,is})} \quad (9)$$

It should be observed that the efficiency reported in Eq. (9) it is not closely correct considering that, due to the machine operation (it happens for all the volumetric machines), part of the expansion ideally happens as an isochoric transformation. Due to this, the ideal power at the denominator tends to decrease, giving an expander higher overall efficiency.

4. Experimental results and numerical validation

In order to experimentally characterize the effects of leakages on the expander performance a wide experimental activity has been developed. To ensure the repeatability of the tests a standard procedure has been adopted as follows:

1. Definition of the ICE working conditions
2. ICE Steady state conditions achievement
3. Setting of the pump rotational speed in order to meet the desired values of pressure and temperature at the expander inlet
4. Power unit steady state conditions achievement

5. Data acquisition

After the definition of the ICE working conditions a time period of 10 min has been waited for the establishment of the steady state conditions. The component of the ORC-based power unit on the other hand showed lower thermal inertia. For this reason, a shorter time period of 2 min has been waited before proceeding with the data acquisition. Data acquisition period was set to 5 s. Considering

a sampling rate of 4500 Hz and the expander rotational speed fixed at 1500 RPM, this corresponds to 125 expander revolutions with a pressure value measured every 2° of rotation which have been retained suitable for the reconstruction of the indicated cycle. In this way, the indicated cycle measurement allowed the experimental evaluation of the mechanical and volumetric efficiency which can be used for the numerical comparison. The volumetric efficiency η_{vol} was evaluated through Eq. (10) following the same approach claimed in Ref. [22]:

$$\eta_{vol} = \frac{\dot{m}_{in}}{\dot{m}_{WF}} = \frac{N_v V_{int,end} \rho_{int,end} \omega}{\dot{m}_{WF}} \quad (10)$$

Moreover, a CFD predictions run on these machines demonstrated that, during the fluid entrance from pipe to vanes, the temperature remains almost constant: so ρ_{int} can be evaluated knowing the pressure inside the vane (at intake end). This datum is known only through the indicated cycle and allows to estimate the pressure drop during intake phase (otherwise not measurable).

The indicated cycle returns also the measurement of the indicated power via Eq. (6) as the working fluid pressure inside the vane during a cycle is known. Therefore, also the mechanical efficiency can be experimentally evaluated through Eq. (8) as the ratio between the mechanical power measured on the shaft and the indicated cycle assessed from the experimental p-V diagram. The mechanical power measured on the shaft was also introduced in Eq. (9) to evaluate the global expander efficiency η_{exp} .

The experimental expander performance in a wide operational range are reported in Table 4. The data have been obtained through the standard procedure previously discussed. In order to assess the response of the expander at various working conditions, the thermal load has been varied for the different cases producing a different recovered thermal power P_{rec} , resulting in the different values of pressure and temperature at the expander inlet. In fact, the intake pressure varies from 0.92 to 1.18 MPa and the mechanical power produced by the expander is comprised in a range between 471 W and 934 W. The minimum value of aspirated mass flow rate is 0.096 kg/s while the maximum one is 0.200 kg/s. The overall expander efficiency reach values in accordance with literature results and is seriously worsened by the high volumetric losses. In fact, η_{exp} resulted equal to 0.4 when the volumetric efficiency η_{vol} is equal to 0.5 representing the main limit to efficiency growth. As already observed during the testing activity, η_{vol} varied from 0.50 to 0.33: this variation was determined by different operating conditions of the expander.

As Table 4 shows, if the volumetric efficiency decreases, the machine permeability increases as mass flow rate aspirated grows to ensure the same intake pressure value. This is in accordance with results reported in Refs. [26,27] and it is due to the higher volumetric losses. Moreover, the permeability increase leads to a growth of thermal power recovered by the working fluid. Indeed, considering for example case 1 and case 5, they have the same intake pressure but, due to the different volumetric efficiency, P_{rec} for case 1 is 37.4 kW and that of case 5 is 22 kW.

The extra amount of P_{rec} of case 1 is due to the leakages and is largely lost at low thermal source. Nevertheless, a part of this energy surplus is recovered as the higher indicated power of case 1 with respect to case 5 confirms. In fact, the leakages between adjacent vanes produce a partial recovery increasing the mass inside the vanes with respect the ideal case. Their effect can be analyzed in Fig. 3 which shows comparisons of the experimental p-V diagrams of several cases of Table 4 with the same intake pressure and different η_{vol} . In particular, in Fig. 3(a) case 1 and case 5, in Fig. 3(b) case 2 and case 6, in Fig. 3(c) case 3 and case 7 and in Fig. 3(d) case 4 and case 8 were respectively reported. Moreover, in

Table 4
Experimental data of operating condition and expander performance.

Case	1	2	3	4	5	6	7	8	
p_{in}	± 0.03 [MPa]	1.18	1.11	1.05	0.95	1.16	1.08	1.02	0.92
p_{out}	± 0.03 [MPa]	0.44	0.43	0.37	0.32	0.48	0.46	0.45	0.41
ω	± 1 [RPM]	1550.3	1546.7	1546.7	1540.7	1536.6	1532.8	1529.2	1524.6
T_{in}	± 0.3 [K]	355.2	351.2	349.3	356.5	369.6	363.9	351.8	347.7
T_{out}	± 0.3 [K]	335.6	333.8	330.9	336.0	351.7	345.2	335.0	327.2
P_{mec}	$\pm 0.8\%$ [W]	934.7	859.1	863.9	795.0	693.3	615.5	559.0	471.4
P_{ind}	$\pm 2\%$ [W]	1104.9	1068.8	1022	866.3	834.4	744	688.7	571.4
P_{rec}	$\pm 0.5\%$ [kW]	37.4	34.1	30.5	27.1	22	20.2	18.7	16.4
\dot{m}_{WF}	$\pm 0.15\%$ [kg/s]	0.200	0.184	0.166	0.138	0.120	0.112	0.110	0.096
η_{vol}	$\pm 2.3\%$	0.33	0.33	0.33	0.33	0.43	0.45	0.45	0.50
η_{exp}	$\pm 1\%$	0.31	0.32	0.32	0.32	0.39	0.39	0.40	0.39

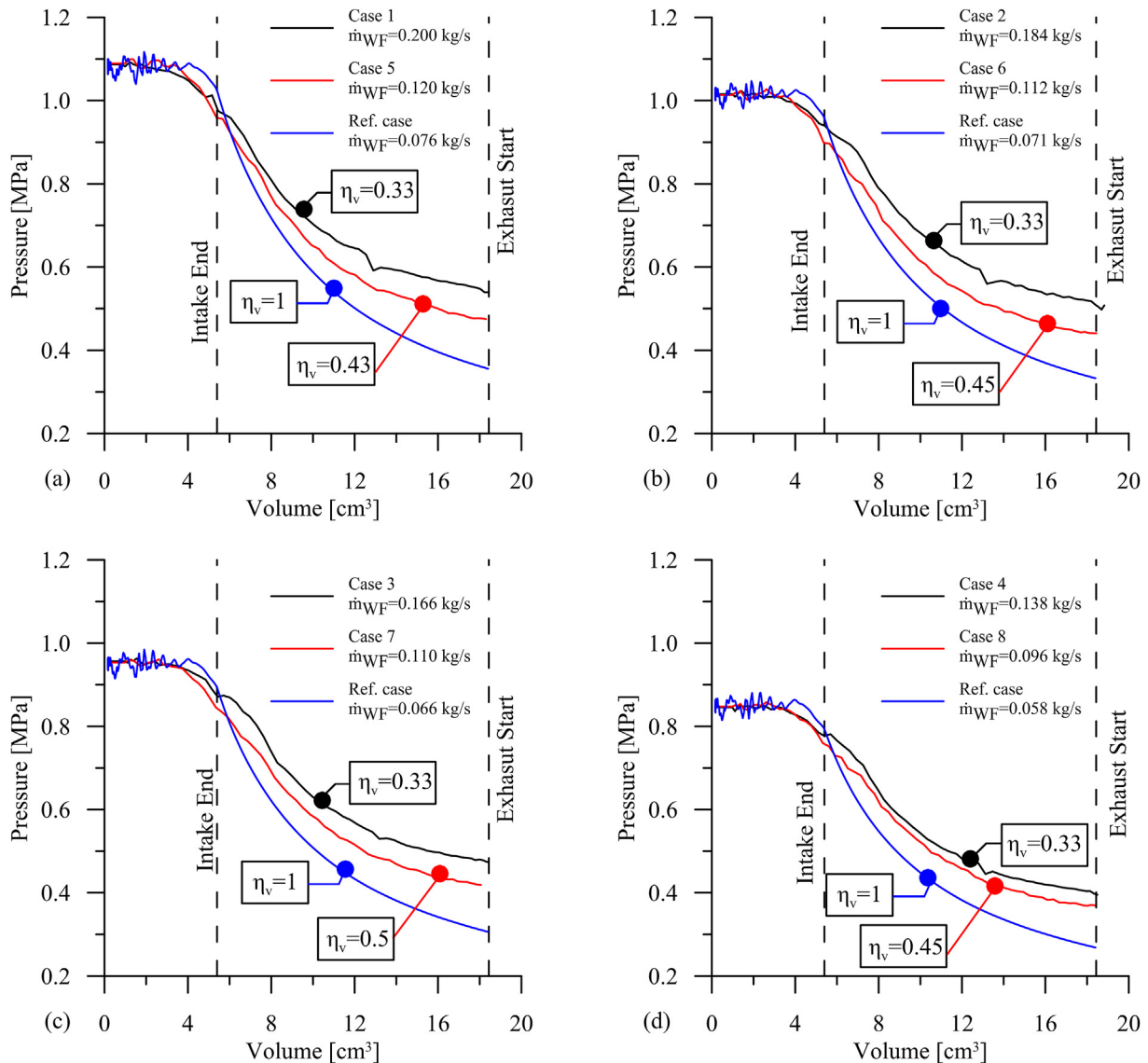


Fig. 3. Experimental indicated cycles for $\eta_{vol} = 0.5$, $\eta_{vol} = 0.33$ and reference case $\eta_{vol} = 1$: (a) Case 1 and Case 5; (b) Case 2 and Case 6; (c) Case 3 and Case 7; (d) Case 4 and Case 8.

Fig. 3 the indicated cycle with the expander affected by absence of leakages ($\eta_{vol} = 1$) has been also shown: this theoretical behavior will correspond to a reference case.

In Fig. 3(a) for a vane intake pressure of 1.08 MPa when η_{vol} is equal to 0.5 the expander requires a \dot{m}_{WF} equal to 120 g/s while, for $\eta_{vol} = 0.33$, \dot{m}_{WF} was equal to 200 g/s. For the reference case \dot{m}_{WF}

was 76 g/s. The difference between \dot{m}_{WF} and the value corresponding to the reference case escapes across the gaps; part of it reaches adjacent vanes increasing their pressure. This explains the lower pressure decrease evident in Fig. 3(a) with respect to the reference case. So, the differences between the real and the reference expansions result amplified by the decrease of volumetric

Table 5
Relative error between predicted and experimental data.

Case	1	2	3	4	5	6	7	8
m_{WF}	2.6%	0.2%	-3.6%	-9.2%	-2.9%	-2.9%	-1.2%	-3.8%
P_{ind}	9.9%	17.9%	7.1%	-3.7%	4.3%	5.4%	9.4%	4.4%
P_{mec}	3.1%	7.7%	-0.8%	-4.2%	-2.4%	-0.9%	2.4%	-0.9%

efficiency. It is worthy to notice how the decrease of η_{vol} delays the closure of the intake port in accordance with literature results [26]. In fact, as Fig. 3(a) shows for experimental case the start of expansion phase does not take place exactly at the end of the intake phase but it is delayed the lower the η_{vol} . It could be observed also that a similar behavior is presented when the upstream pressure of the expander decreases, Fig. 3(b)–(d). From the data it is also clear that when the exhaust starts, a higher pressure level is inside the vanes and this prevents the eventual backflows that can happen, strongly reducing the produced work, if the base pressure is greater than the vane value.

In order to assess the role of leakages, the developed numerical model has been used to predict the flow rates moving between different vanes. The model reproduces very closely the experimental performance (Table 5), including the variations of volumetric efficiency η_{vol} : so, it can be considered as a very fine virtual platform.

Table 5 shows very low relative errors in terms of mass flow rate, indicated and mechanical power between predicted and real data. The model reproduces with good accuracy also the indicated diagrams (p-V) as it is clearly shown in Fig. 4.

As the clearance at the tip blade δ (Eq. (2)) was hardly measurable, it was identified thanks to a calibration procedure. The best calibration parameter was offered by the difference between the measured mass flow rate and the reference value. Table 6 shows the resulting equivalent clearances. When the η_{vol} of the machine is 0.50 δ is estimated equal to 85 μm while when the η_{vol} decreases up 0.33 δ is 170 μm . Of course in the reference case ($\eta_{vol} = 1$) clearance should be zero but, in order to avoid mathematical errors, a very low value has been used (10 μm). Despite the main effects on expander performance was exerted by leakages across the vane at tip blade, for the sake of completeness in Table 6 also the gap between rotor and end-wall plate and between vane side and rotor slot have been reported.

6. Analysis of leakage impact on flowrate among vanes

In order to understand the effects of the volumetric losses on the expander performance, two cases in which the expander has different clearances between vane tip and stator were analyzed. In the first case η_{vol} is equal to 0.50 and the corresponding clearance is 85 μm (Table 6); the second case is represented by the reference case (nil leakages, 10 μm clearance). In Fig. 5(a), for each θ value it is evident that the pressure referred to a higher clearance is greater than the value with a lower clearance: this can be only due to the mass increase inside the vane due to leakages. Moreover, the two situations require different mass flow rate aspirated by the machines, as it is shown in Fig. 5(b): two different average values characterize the two machines (0.067 kg/s for the reference case and 0.131 kg/s for that with gap of 85 μm) and unsteadiness are also evident during vane filling (when the blade crosses the port the flow rate sharply decreases due to the partial obstruction of it). In Fig. 5(c) and (d) the actual mass (inside the vane) and the mass flow rate entering the vanes during the expansion are respectively represented. Mass inside the vanes grows when the clearance is 85 μm after the intake port closing and this means that it is fed by the leakages from surrounding vanes (Fig. 5(c)). This doesn't happen in the ideal case where, after the intake port closing, the mass inside remains almost constant: just after the exhaust port opening, in the reference case, the pressure inside the vane is lower than the exhaust pressure outside of the vane Fig. 5(a) and a strong backflow happens (Fig. 5(c)) as it is demonstrated also in Fig. 5(d). When leakages are present, the filling/emptying of the vane is a quite complex phenomenon. Considering the filling process, it is useful to consider the three vanes reported in Fig. 6 in which Vane 1 (V1) is the one directly filled through the intake port, Vane 2 (V2) is the one which follows (according to the revolution speed), Vane 7 (V7) is the vane which passed before. According to the instantaneous pressures inside V1, V2, V7 leakages happen further filling or emptying V1. As can be seen from Fig. 5, the leakages are considered positive if they flow into V1.

With reference to the machine having η_{vol} equal to 0.50, Fig. 7(a) shows the pressure values inside the three vanes as a function of θ . Obviously, the 3 pressure behaviors are sequentially phased of an angular value equal to the vane angular extent $\Delta\theta_{vane}$ (51.4°). In Fig. 7(b) the same representation is given for the reference case.

Fig. 8(a) and (b) show, respectively, the mass flow rate which passes through the intake port moving towards the vane for the

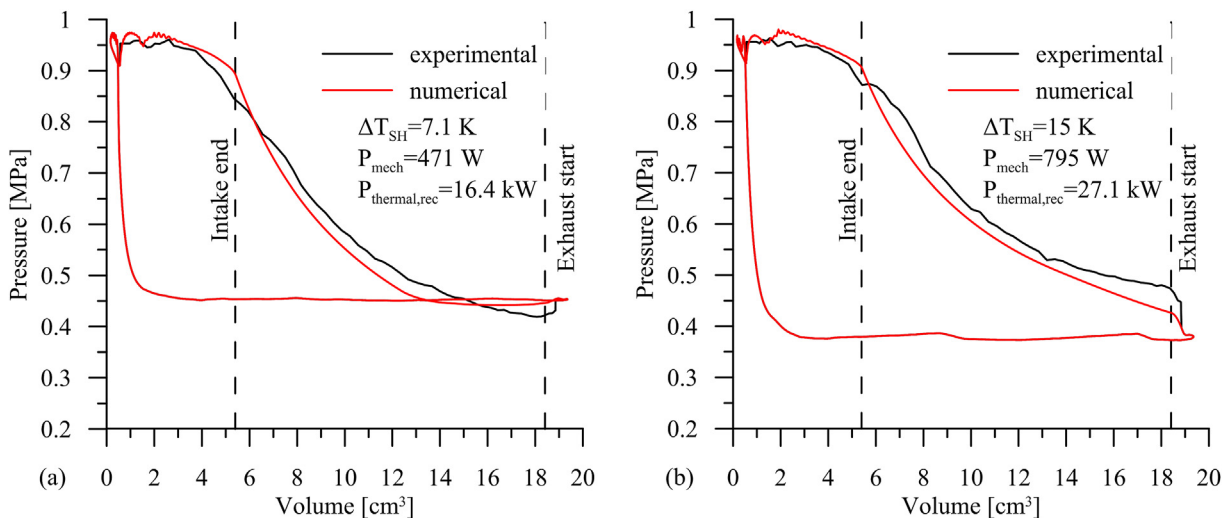


Fig. 4. Experimental and predicted indicated cycle: (a) Case 7 of Table 4; (b) Case 3 of Table 4.

Table 6
Estimated and assumed clearances.

Volumetric Efficiency η_{vol}	0.50	0.33
Clearance between vane tip and stator δ	85 μm	170 μm
Clearance between vane side and rotor slot δ'	5 μm	5 μm
Clearance between rotor and casing (equivalent diameter) D_{covers}	0.2 mm	0.2 mm

machine with η_{vol} equal to 0.50 and for the reference case. The intake phase start when θ is equal to 342.7° while ends at 71° . The exhaust phase is showed in Fig. 8(c) for the real case and in Fig. 8(d) for the reference one. The exhaust phase starts at 157° and ends at 348.2° .

The mass flow rate through the intake and exhaust ports are the main contributes which respectively fill and empty V1 but they are not the only ones. In fact, two others contributions referring to the flow rate exchanged with V7 and V2 due to blade tip leakages should be considered in the evaluation of the mass inside V1. These contributions depend on the phase performed by the expander,

thus referring to Fig. 9 the following considerations apply:

- a) Intake phase of V1: Concerning the mass flow rate $\dot{m}_{leak,1}$ exchanged with V7, except for the angular extent between 342.7° and 18° , the pressure inside V1 is always higher as it is aspirating while V7 is expanding (Fig. 7(a)). Therefore, the leakages are negative as can be noticed in Fig. 9(a). So, part of the mass flow rate introduced inside V1 flows towards V7. A similar behavior is shown by the mass exchanged with V2, $\dot{m}_{leak,2}$ (Fig. 9(b)). In fact, for θ in a range within 342.7° and 34° , the pressure of V2 is lower than that in V1 so the $\dot{m}_{leak,2}$ flows from

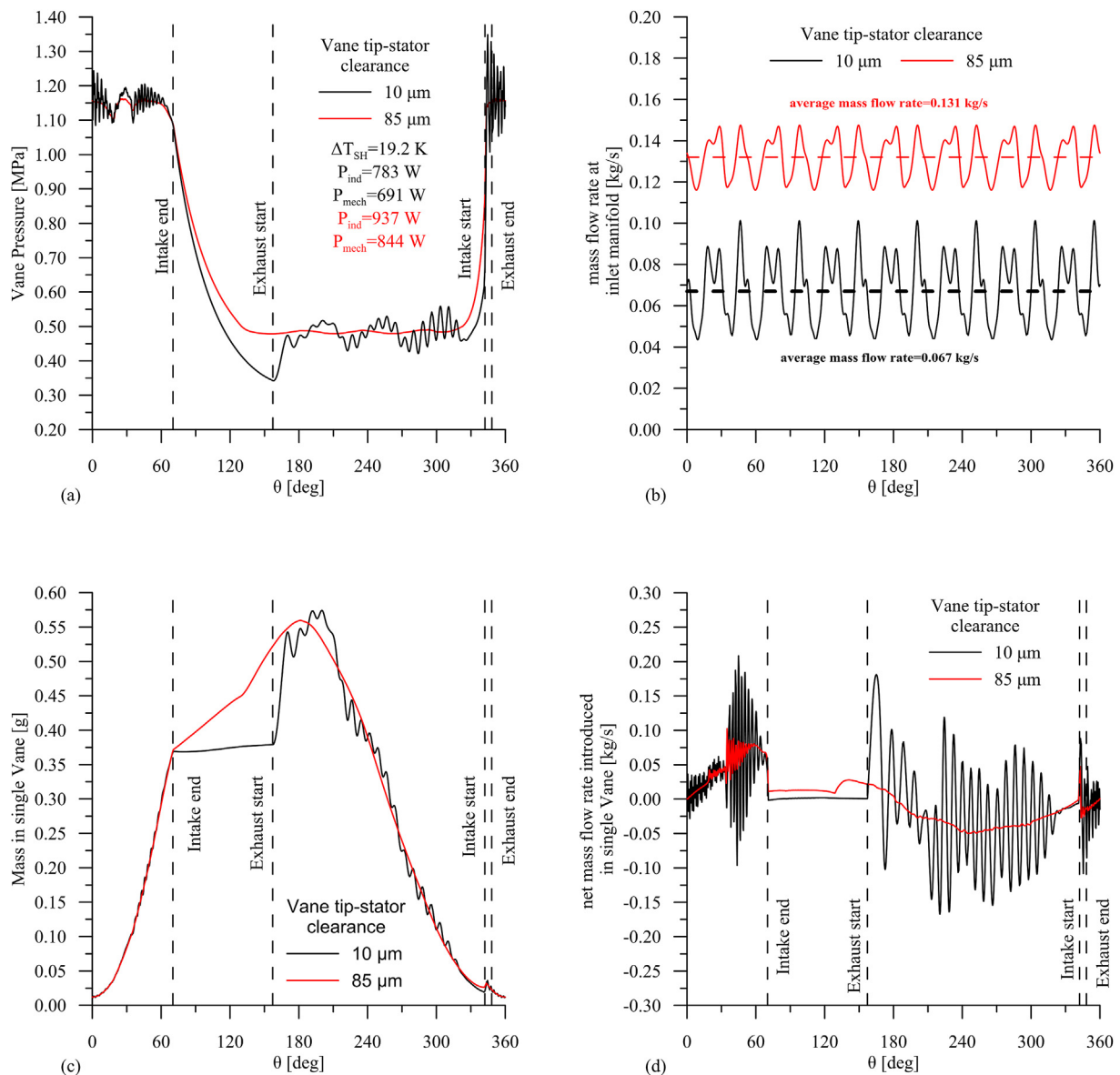


Fig. 5. (a) p- θ diagram; (b) expander inlet mass flow rate; (c) actual vane mass (d) net mass flow rate inside vane.

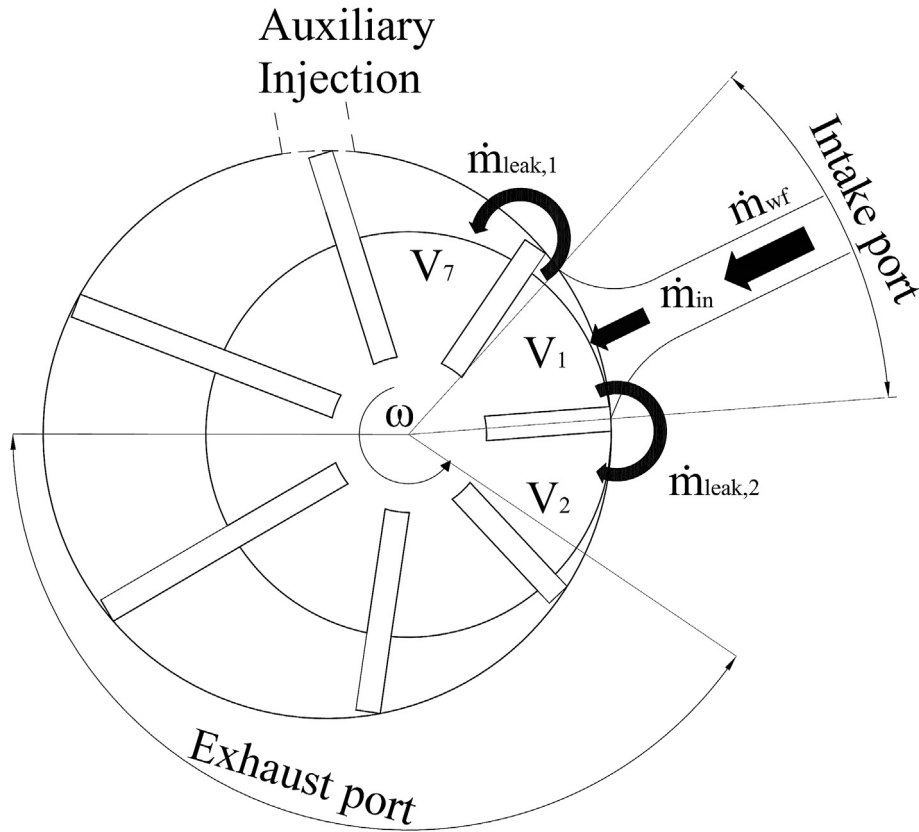


Fig. 6. Scheme of flow leakages between vane tip and inner stator surface.

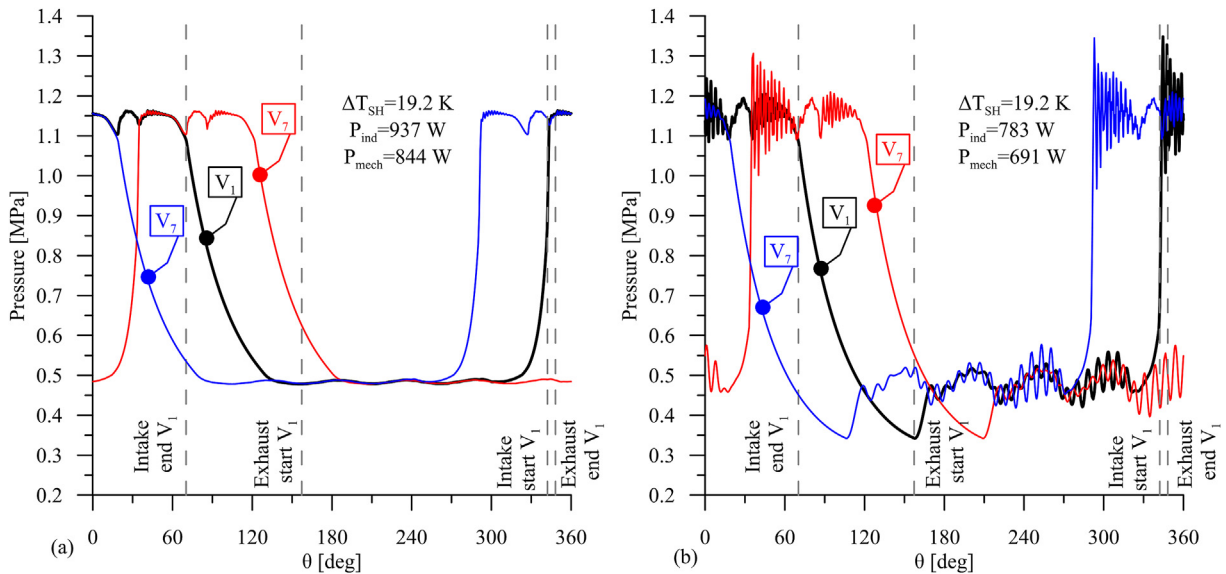


Fig. 7. angular phasing of p-θ diagram of adjacent vanes for clearance between blade tip and stator equals to 85 μm (a) and 10 μm (b).

V1 to V2. Thus, during the intake phase of V1, the leakages towards V7 and V2 worsen the filling of V1 itself.

b) Expansion phase of V1: during the expansion phase the pressure inside V1 is higher than that in V7 but it is lower than that in V2 (Fig. 7(a)). Thus, the mass flow exchanged with V7 ($\dot{m}_{leak,1}$) is negative so the working fluid flows from V1 to V7 (Fig. 9(a)). As

Fig. 9(b) shows, an opposite contribution is offered by the mass flow rate from V2 ($\dot{m}_{leak,2}$) which is positive and consequently enters V1. Therefore, during the expansion of V1, the mass inside it increases because the mass flow rate entering the chamber from V2 is higher than the one which leaves it. Fig. 5(c) confirms

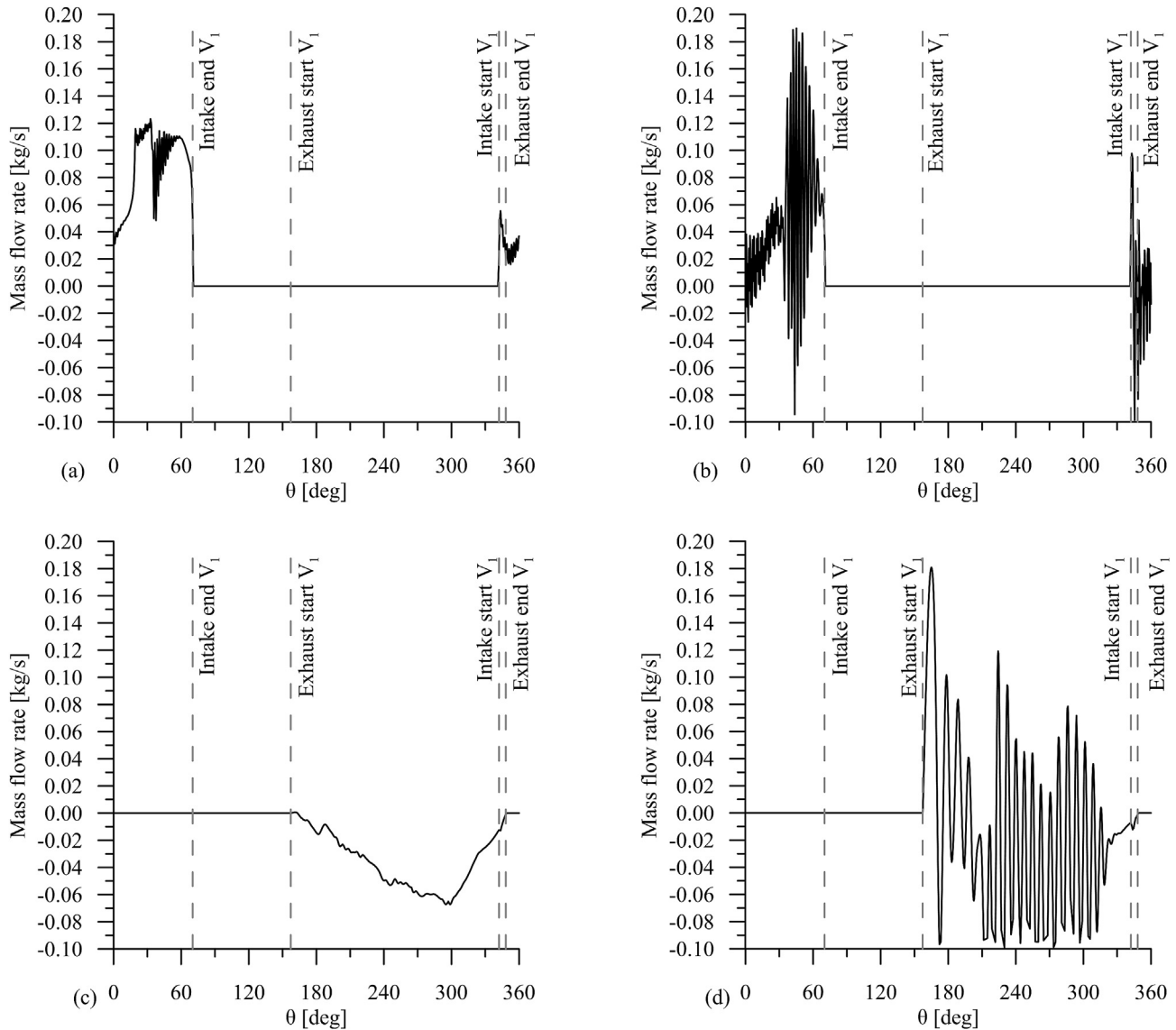


Fig. 8. Mass flow rate at intake port for clearance equals to 85 μm (a) and 10 μm (b). Mass flow rate at exhaust port for clearance equals to 85 μm (c) and 10 μm (d).

this behavior and explains a lower pressure decrease with respect to the ideal case Fig. 5(a).

- c) Exhaust phase of V1: during the exhaust phase, the pressure inside V7 and V2 is higher than that in V1 (Fig. 7(a)) so, both $\dot{m}_{\text{leak},1}$ and $\dot{m}_{\text{leak},2}$ are positive as can be observed in Fig. 9(a) and (b). This means that the leakages from V7 and V2 obstacle the emptying of V1. Moreover, the working fluid flowing towards adjacent chambers towards V1 during its exhaust phase is not useful because it not able to increase the pressure inside that chamber being in communication with the exhaust port.

For the reference case the filling and the emptying processes of the chambers are simpler as they are not affected by the leakages between adjacent chambers. In fact, despite the pressure difference between the adjacent vanes is quite similar with respect to the real case (Fig. 7(b)), the low clearances between blade tip and stator imply that the mass flow rates exchanged between V7 and V1 (Fig. 9(c)) and between V2 and V1 (Fig. 9(d)) are negligible. Hence, V1 is filled and emptied only through the intake port and the exhaust port respectively. Moreover, the absence of leakages

involves that all the mass flow rate provided by the pump enters the vanes and the mass inside them remains constant when the intake port is closed, as can be noticed from Fig. 5(c).

Therefore, the main drivers of the leakages flow between adjacent vane are represented by the clearance gap between the blade and stator surface and the pressure difference between the chambers which relies by design such as vane number and angular positions of intake and exhaust ports. Hence, the type of working fluid selected does not affect the general trend of the vane leakages. Nevertheless, for the same pressure difference between vanes and clearances, the working fluid choice can change the amount of leakages flow. In fact, as Eq. (2) states, the volumetric flow rate depends by the dynamic viscosity μ of the working fluid selected. In particular, the higher is μ the lower is the volumetric leakages flow rate. The working fluid selection can affects also the clearance gap between blade and stator surface due to the tribological interaction with the surfaces. The higher the density of the fluid is, the higher will be the sealing effect produced by the fluid layer – often mixed with some lubricating oil – in contact with the surfaces.

In Fig. 10 the modifications of the indicated cycle due leakages

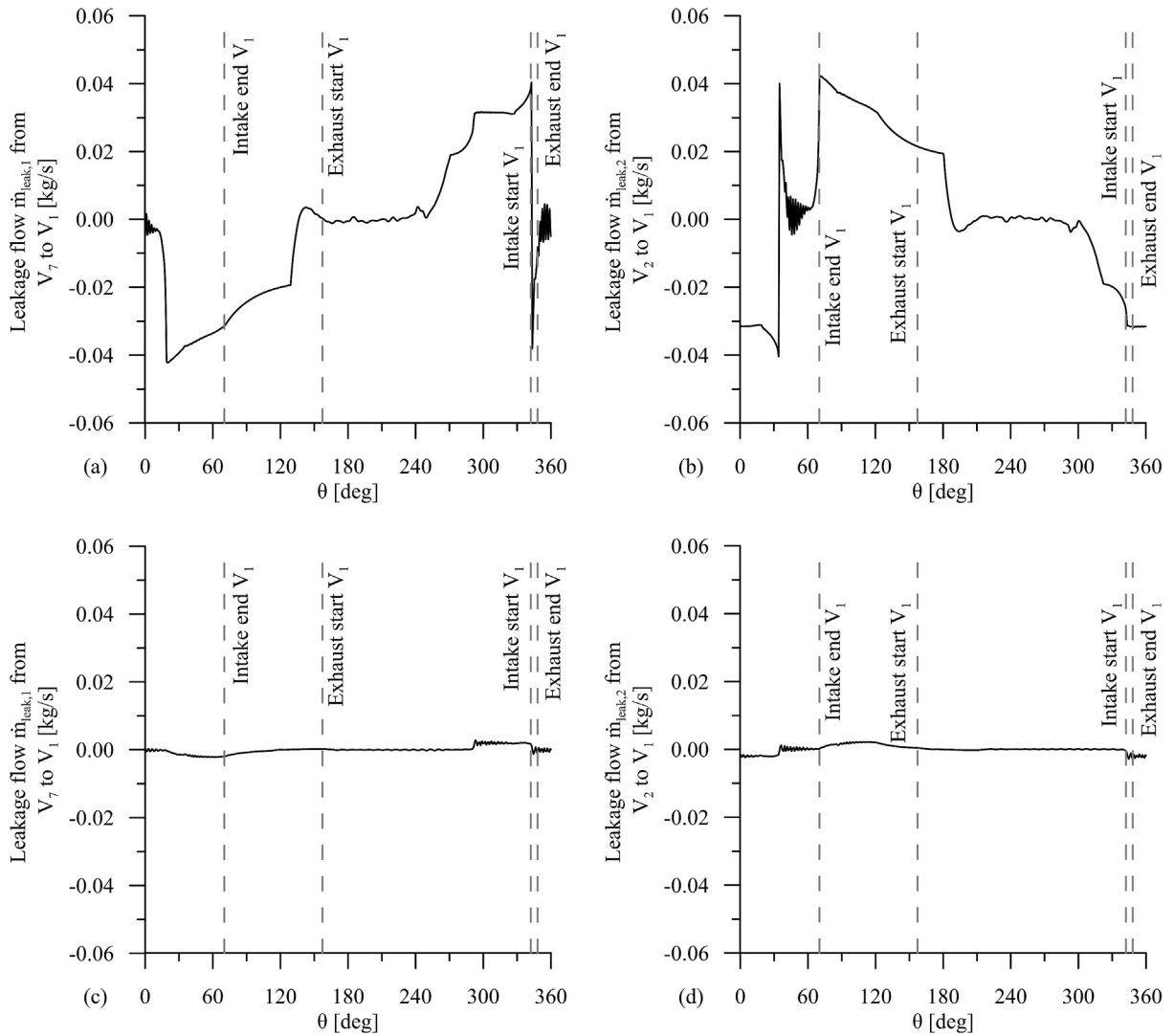


Fig. 9. Leakages between adjacent chambers: (a) from V_7 to V_1 (gap of 85 μm); (b) from V_2 to V_1 (gap of 85 μm); (c) from V_7 to V_1 (gap of 10 μm); (d) from V_2 to V_1 (gap of 10 μm).

has been reported. In particular, three cases were considered:

- 1) Case 1: in Fig. 10(a), referred to a machine having a $\eta_{vol} = 0.50$;
- 2) Case 2: in Fig. 10(a), referred to the reference expander ($\eta_{vol} = 1$);
- 3) Case 3: in Fig. 10(b), referred to a larger ideal machine ($\eta_{vol} = 1$) whose design mass flow rate equals that provided by the pump in the Case 1.

The intention of the comparison among these cases is to demonstrate the influence of the volumetric losses on the indicated power. All the indicated cycles are reported for the same upstream pressure; Case 3, of course, refers to a larger machine. The difference between the indicated cycles of Case 1 and Case 2 is represented by the “A” area: the two machines aspirate different flow rates and, in the real machine, part of it is transformed in leakages, but they increase the pressure inside the vane and produce more work. The “A” area is equal to 13.5% of work referred to Case 2. So Case 1 has a greater mass flow rate (60% more than case 2) but it presents a work recovery 13.5% greater than Case 2. Increasing the size of the expander with a volumetric efficiency close to 1, the indicated power increases of a factor given by the ratio between the

two flow rates. It is evident how leakages break this proportionality. The same analysis were repeated increasing the back-pressure at the expander’s exit. The results showed that the amount of recovery is amplified when the backpressure increases from 0.37 MPa (Fig. 10(a) and (b)) to 0.43 MPa (Fig. 10(c) and (d)). In this case, the area “A” is the 16.6% of the work referred to Case 2. Indeed, the higher pressure inside the vanes during the expansion produces a higher pressure when the discharge port opens, preventing a backflow at the exhaust port. Table 7 reports a summary of the indicated power increase due to the presence of leakages.

Thanks to the obtained results, the leakages between adjacent vanes can be seen under a new light with respect to actual knowledge. Even if their negative effects on overall expander efficiency are confirmed, some positive aspects can be found. In fact, leakages sustain the pressure beyond the intake port closure leading to a modification in expander volume ratio allowing to deal with an outlet pressure increase.

7. Effects of dual-intake port technology on expander filling

The dual-intake-port technology allows to increase the indicated and the mechanical power of the expander for the same

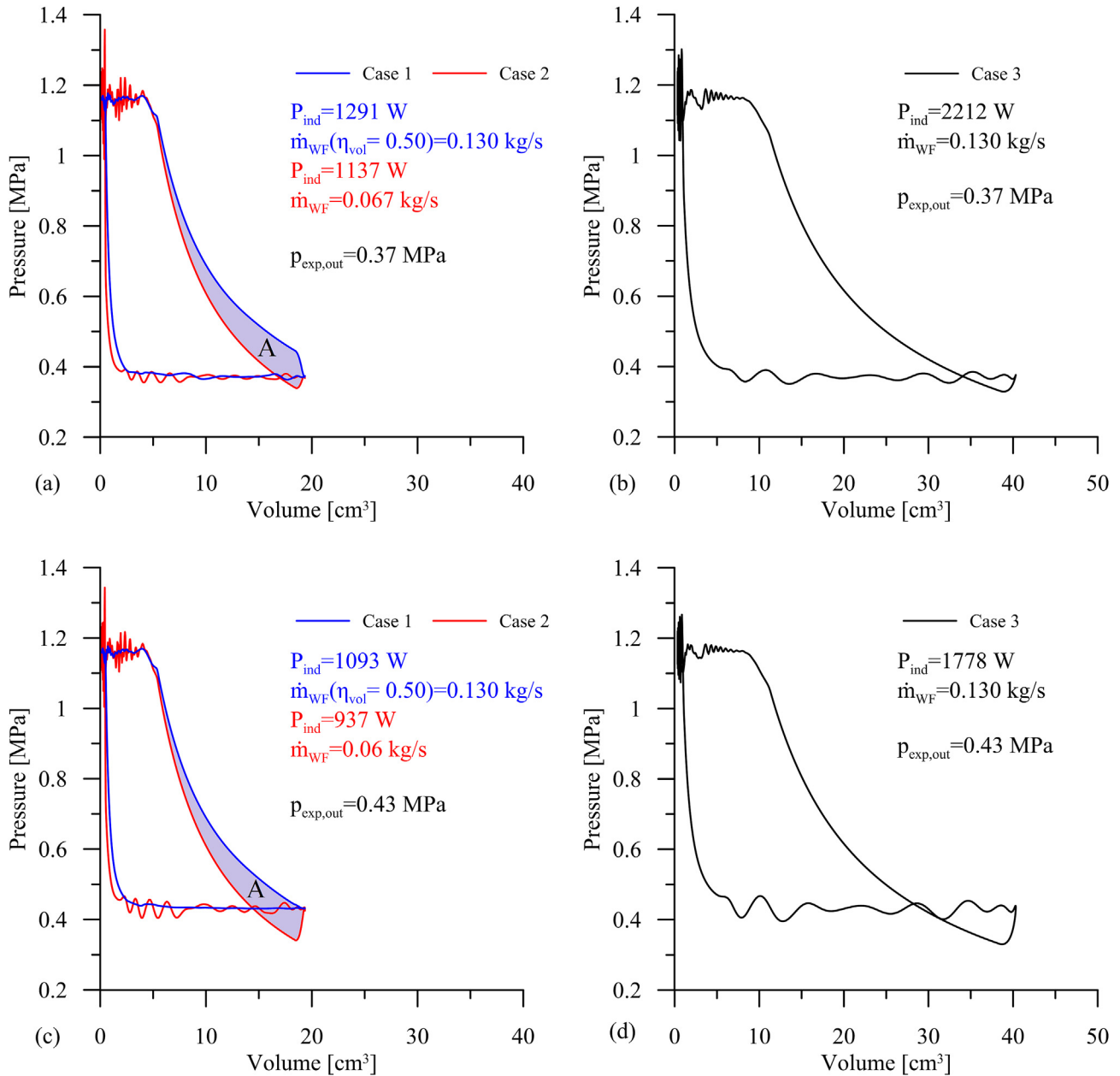


Fig. 10. (a) Case 1 and case 2 ($p_{\text{exp,out}} = 0.37$); (b) Case 3 ($p_{\text{exp,out}} = 0.37$); (c) Case 1 and case 2 ($p_{\text{exp,out}} = 0.43$ MPa); (d) Case 3 ($p_{\text{exp,out}} = 0.43$ MPa).

Table 7

Indicated power recovery due to vane leakages.

	$p_{\text{exp,out}} = 0.37$ MPa, Fig. 10(a)	$p_{\text{exp,out}} = 0.43$ MPa, Fig. 10(c)
Area A	154 W	156 W
P_{ind} recovery (% of P_{ind} of Case 2)	13.5%	16.6%

intake pressure with respect to the conventional single intake port machine, [32]. Concerning the role of leakages, an additional positive contribution can be observed. As shown in Fig. 11, the dual intake port position $\Phi_{\text{dual int}}$ is defined as the difference between the starting angle of the secondary intake port $\theta_{\text{dual int,start}}$ and the ending angle of the intake one $\theta_{\text{int,end}}$. For the expander under consideration, the angular extent of dual port $\Delta\theta_{\text{dual int}}$ is equal to 12° . The second port has an extension equal to 15% of the main one.

In Table 8 the effects of $\Phi_{\text{dual int}}$ on leakages across vane from V1

to V7 and to V2 were reported. Moreover, the benefits introduced by dual intake technology on the produced mechanical power and expander efficiency were shown. The overall efficiency of the dual intake port expander is higher than the single port one for all the values of $\Phi_{\text{dual int}}$ considered and it reaches a maximum when the circumferential position is located close to 15° . The maximum produced power and aspirated mass flow rate occur for $\Phi_{\text{dual int}}$ close to 65° in correspondence to which the volume of the vane is close to its maximum. These results are in accordance to the

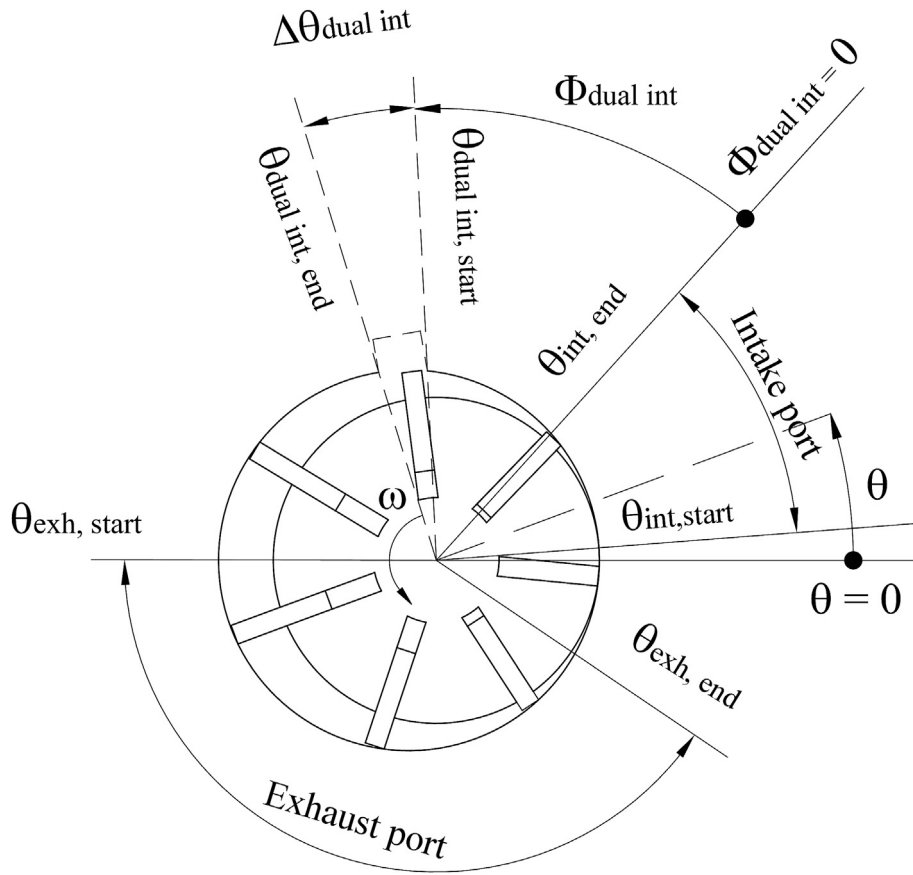


Fig. 11. Scheme of the dual intake port expander.

Table 8
Effects of dual intake port on expander performance varying $\Phi_{\text{dual int}}$.

$\Phi_{\text{dual int}}$ [deg]	$\dot{m}_{\text{leak V2} \rightarrow \text{V1}}$ [kg/s]	$\dot{m}_{\text{leak V1} \rightarrow \text{V7}}$ [kg/s]	\dot{m}_{wf} [kg/s]	Impact of leakages on \dot{m}_{wf} [%]	P_{mech} [W]	η_{mech}	η_{vol}
Single-intake	0.003	0.003	0.132	2.5%	844	0.90	0.43
1.3	0.006	0.006	0.160	3.7%	1251	0.93	0.55
8.4	0.006	0.006	0.174	3.5%	1405	0.93	0.55
15.4	0.006	0.006	0.191	3.4%	1554	0.94	0.55
22.4	0.007	0.007	0.206	3.2%	1674	0.94	0.55
29.5	0.006	0.006	0.222	2.9%	1770	0.94	0.53
36.5	0.006	0.006	0.237	2.6%	1841	0.94	0.52
43.6	0.006	0.006	0.249	2.2%	1882	0.95	0.51
50.6	0.004	0.004	0.260	1.6%	1905	0.95	0.49
57.7	0.003	0.003	0.270	1.0%	1917	0.95	0.47
64.7	0.001	0.001	0.279	0.4%	1913	0.95	0.46

efficiency and power benefits reported in Ref. [32]. Table 8 shows also a further benefits of this technology never observed before: the dual-intake port for proper $\Phi_{\text{dual int}}$ reduces leakages nonetheless this technology involves the increase of mass flow rate aspirated to pull up the mechanical power. Indeed, the leakages between adjacent chambers decrease up to 65% with respect to single intake expander. Moreover, the impact of the leakages, defined as the ratio between the corresponding mass flow rates through adjacent vanes and that provided by the expander, decreases from 2.5% in the single intake machine to 0.4% in the dual intake port one when $\Phi_{\text{dual int}}$ equals to 65°. A reduction of the impact of leakages on the whole mass flow rate is still achieved for all $\Phi_{\text{dual int}}$ comprised between 43.6° and 65°. Higher angle than 65° are not considered because the dual intake phase are overlapped with the discharge one worsening the expander performance, [32]. The leakages

reduction is due to the lower extent of vane pressure difference in dual intake expander as shown in Fig. 12 where the pressure differences between V1 and V7 are reported for the single (Fig. 12(a)) and dual intake port (Fig. 12(b)).

In Fig. 12(a) the p-θ cycles of two adjacent vanes have been reported for the single-port expander. The intake phase of V1 starts at $\theta = 341.2^\circ$ and ends at $\theta = 71^\circ$ while its exhaust phase starts for $\theta = 157^\circ$ and ends when $\theta = 348.2^\circ$. Concerning V7, as it precedes V1 (according to expander rotation), its intake and exhaust phase are anticipated by a vane angular extent $\Delta\theta_{\text{vane}}$. Therefore, the intake phase of V7 starts for a $\theta = 291.3^\circ$ and ends when $\theta = 19.6^\circ$. Similarly, the exhaust phase starts at $\theta = 105.6^\circ$ and ends at $\theta = 296.8^\circ$. Thus, the angular shift between two indicated cycles produces a pressure difference between the vanes. In particular, two regions can be recognized (Fig. 12):

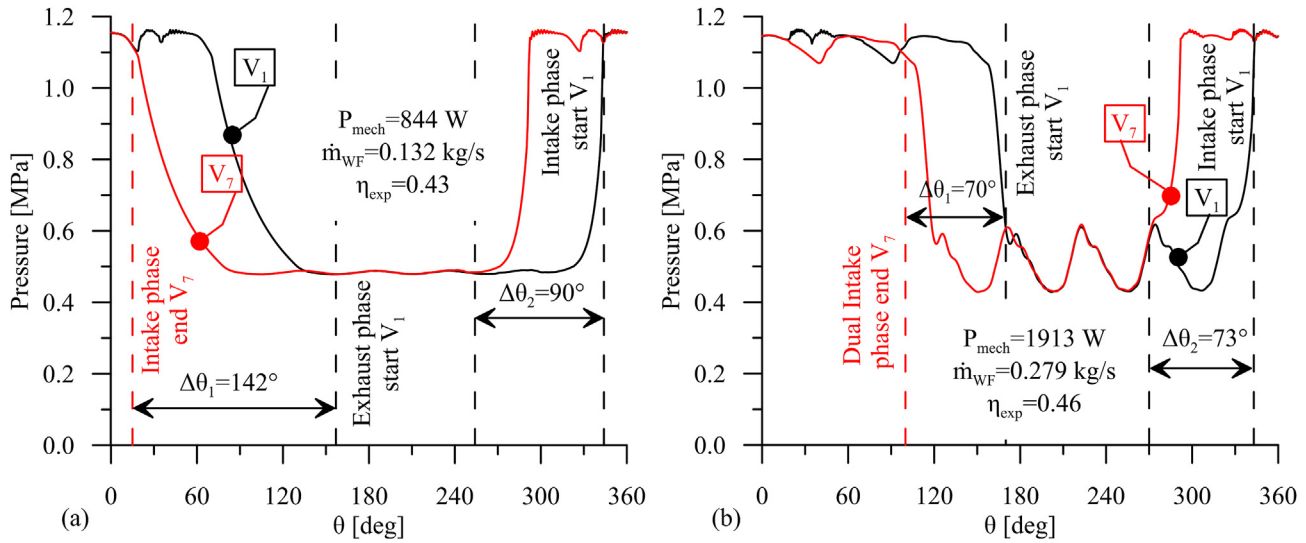


Fig. 12. Pressure difference between adjacent chambers for conventional (a) and dual-intake port expander for $\Phi_{dual\ int} = 65^\circ$ (b).

- a) $\Delta\theta_1$: In this angular region V7 performs the expansion and the exhaust phase while V1 aspirates and subsequently expands. During $\Delta\theta_1$ the pressure inside V1 is always higher than that in V7. For the single intake expander $\Delta\theta_1 = 142^\circ$.
- b) $\Delta\theta_2$: In correspondence of this angular extent, V1 completes its exhaust phase and subsequently starts to aspirate while V7 performs the intake phase after the conclusion of the exhaust. Thus, during $\Delta\theta_2$ the pressure inside V7 is always higher than that inside V1. This angular extent is equal to 90° and it is higher than the angular extent from the start of the intake phase of V7 ($\theta_{int,start} = 291.4^\circ$) till to the end of the exhaust phase of V1 (342.8°). This is due to the recompression of residual fluid inside V7 before the start of its intake phase, as the chamber volume is very small in the last part of discharge.

The introduction of an auxiliary intake port modifies the angular extension of $\Delta\theta_1$ and $\Delta\theta_2$. In Fig. 12(b) the p - θ of V1 and V7 for dual intake port expander with $\Phi_{dual\ int}$ equals to 65° were reported. The main intake and the exhaust phases of the expander are equal to those of the single intake port. More in particular, as the $\Phi_{dual\ int}$ is equal to 65° , the second intake phase starts when θ is equal to 90° and ends for θ equals to 153.4° . Therefore, the second intake phase ensures a quite constant pressure inside the vane despite the higher volume of the chamber. In fact, the dual intake phase prevents the expansion of the working fluid which takes place only for a small angular extent (20°) between the end of the main intake phase and the start of the second one. Moreover, the pressure difference in this angular region between V1 and V7 is very low and it does not lead to a significant mass exchange between the chambers. Therefore, the dual intake port modifies $\Delta\theta_1$ and $\Delta\theta_2$:

- $\Delta\theta_1$ is equal to 70° and it is lower than the value of the single intake expander (142°). During $\Delta\theta_1$, V1 is aspirating through the dual intake port while V7 is discharging, so the pressure inside it is lower than that in V1;
- $\Delta\theta_2$ is equal to 73° and it is close to that of single-intake port expander (90°) because the starting and ending angles of the exhaust phase are equal for the two machines.

Therefore, under the same working conditions (upstream pressure), the two adjacent chambers of the dual port expander have a pressure difference of the same magnitude with respect the

OEM machine but for a lower angular extent. This aspects leads to a decrease of the leakages across the vanes when the clearances are the same for both machines.

In Fig. 13, the net effect of the reduction of the leakages associated with the dual intake port machine technology is reported. The mass flow rate from V7 to V1 and that from V2 to V1 are shown for single (Fig. 13(a) and b)) and dual intake expander (Fig. 13(c) and (d)) with $\Phi_{dual\ int} = 65^\circ$. They are higher for the single-intake expander with respect to the dual-intake port type. The dual-intake port machine modifies the pressure difference between adjacent vanes, reducing $\Delta\theta_1$ and "breaking" the increase of leakages which happens for the OEM machine.

Therefore, the dual-intake-port expander can be successfully used to improve the filling phase of the machine. This novel technology opens the way to a new concept of vane leakage reduction. In fact, according to the current design choice proposed in literature, volumetric efficiency is improved increasing the number of the vanes [38] and/or increasing the reaction force at the tip blades [22]. This is beneficial in terms of volumetric efficiency but it is detrimental in terms of mechanical losses: part of the benefits are, therefore, reduced. Differently, dual-intake-port technology intrinsically reduced leakages without worsening expander mechanical efficiency.

8. Conclusions

In the present work a characterization of the effects of the leakages inside a sliding rotary vane expander has been studied. The indicated cycle and all the other measurements on the plant allowed to validate a mathematical model of the expander in order to represent flow leakages inside the machine at tip blades, the most relevant contribution. The experimental and numerical analysis demonstrated that:

- If the volumetric efficiency of the expander decreases, in order to ensure the same intake pressure, the mass flow rate of the working fluid provided by the pump must grow, to compensate the leakage losses;
- Most part of the leakages occurs between vanes at the vane tip; the leakages at vane side and between the rotor and end wall plate are one order of magnitude lower;

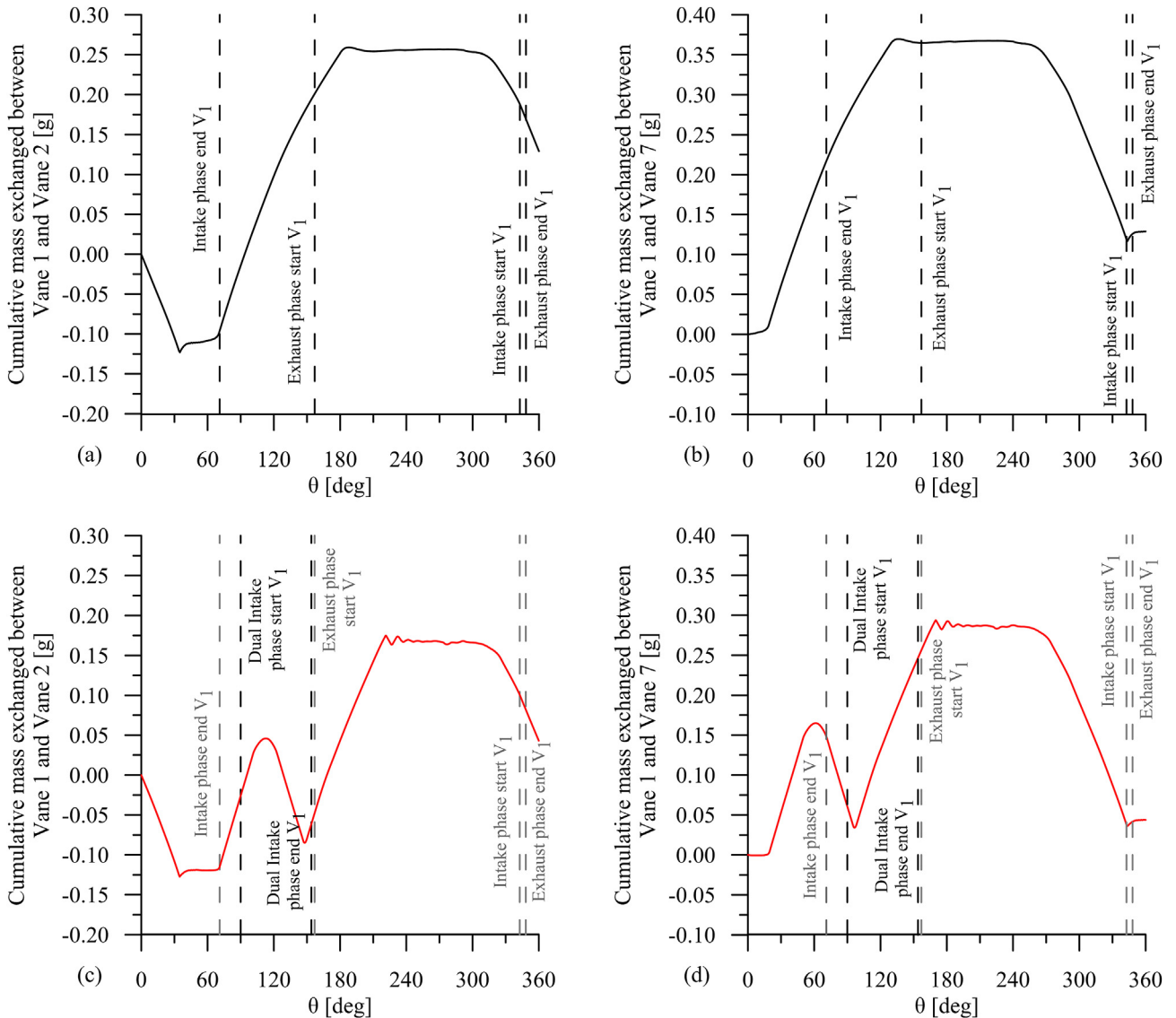


Fig. 13. Leakages between V_1 and V_2 (a), V_1 and V_7 (b) of OEM expander and between V_1 and V_2 (c) and V_1 and V_7 (d) of dual intake port expander ($\Phi_{\text{dual int}} = 65^\circ$).

- The p-V curve is strongly influenced by the leakages: when the volumetric efficiency decreases, the pressure inside the vane is sustained by the leakages. In fact, the fluid which escapes across the clearances increases the pressure inside the adjacent vanes. This fact produces an increase in the indicated work and, in a certain sense, this effect can be seen as a partial recovery of the volumetric efficiency decrease; The recovery grows up to 16.6% of the work produced by an ideal machine characterized by an adiabatic isentropic transformation;
- A volumetric efficiency increase can be reached by decreasing the gap between tip blade and stator surfaces but this will increase the friction power, so decrease the mechanical efficiency of the machine. These conclusions allowed to reinforce the validity of a new technology already discussed by the Authors represented by the use of a dual-intake port angularly spaced from the main one, both fed at the same pressure. According to this, the volumetric efficiency of the dual-intake-port machine is improved also because leakages among vanes are reduced up to 60–70% with respect to the single intake machine.

Acknowledgments

The authors are grateful to Ing. Enea Mattei S.p.A, its CEO, Dr. Giulio Contaldi, and Dr. Stefano Murgia for the support given during this research activity.

Appendix A. Supplementary data

Supplementary data to this article can be found online at <https://doi.org/10.1016/j.energy.2019.116721>.

References

- [1] Teng H, Regner G, Cowland C. Waste heat recovery of heavy-duty diesel engines by organic Rankine cycle Part I: hybrid energy system of diesel and Rankine engines. SAE Technical Paper 2007:1–537.
- [2] Teng H, Regner G, Cowland C. Achieving high engine efficiency for heavy duty diesel engines by waste heat recovery using supercritical organic-fluid Rankine cycle. SAE Paper 2006:1–3522.
- [3] Anna Chatzopoulou Maria, Lecompte Steven, De Paepe Michel, Markides Christos N. Off-design optimisation of organic Rankine cycle (ORC) engines with different heat exchangers and volumetric expanders in waste heat recovery applications. Appl Energy 2019;253:113442. <https://doi.org/>

- 10.1016/j.apenergy.2019.113442. ISSN 0306-2619.
- [4] Pantano Fabio, Capata Roberto. Expander selection for an on board ORC energy recovery system. *Energy* 2017;141:1084–96. <https://doi.org/10.1016/j.energy.2017.09.142>. ISSN 0360-5442.
 - [5] Song Panpan, Wei Mingshan, Zhang Yangjun, Sun Liwei, Emhardt Simon, Zhuge Weilin. The impact of a bilateral symmetric discharge structure on the performance of a scroll expander for ORC power generation system. *Energy* 2018;158. <https://doi.org/10.1016/j.energy.2018.06.053>. ISSN 0360-5442, 458-470.
 - [6] Luis Eric Olmedo, Mounier Violette, Mendoza Luis Carlos, Schiffmann Jürg. Dimensionless correlations and performance maps of scroll expanders for micro-scale Organic Rankine Cycles. *Energy* 2018;156:520–33. <https://doi.org/10.1016/j.energy.2018.05.001>. ISSN 0360-5442.
 - [7] Pantaleo AM, Simpson M, Rotolo G, Distaso E, Oyewunmi OA, Sapin P, De Palma P, Markides CN. Thermo-economic optimisation of small-scale organic Rankine cycle systems based on screw vs. piston expander maps in waste heat recovery applications. *Energy Convers Manag* 2005;2019:112053. <https://doi.org/10.1016/j.enconman.2019.112053>. ISSN 0196-8904.
 - [8] Shen Lili, Wang Wei, Wu Yuting, Cheng Liang, Lei Biao, Zhi Ruiping, Ma Chongfang. Theoretical and experimental analyses of the internal leakage in single-screw expanders. *Int J Refrig* 2018;86:273–81. <https://doi.org/10.1016/j.ijrefrig.2017.10.037>. ISSN 0140-7007.
 - [9] Shen Lili, Wang Wei, Wu Yuting, Lei Biao, Zhi Ruiping, Lu Yuanwei, Wang Jingfu, Ma Chongfang. A study of clearance height on the performance of single-screw expanders in small-scale organic Rankine cycles. *Energy* 2018;153:45–55. <https://doi.org/10.1016/j.energy.2018.02.004>. ISSN 0360-5442.
 - [10] Xia Chunli, Zhang Wei, Bu Gaoxuan, Wang Zhizhong, Shu Pengcheng. Experimental study on a sliding vane expander in the HFC410A refrigeration system for energy recovery. *Appl Therm Eng* 2013;59(1–2):559–67. <https://doi.org/10.1016/j.applthermaleng.2013.05.050>. ISSN 1359-4311.
 - [11] Musthafah MT, Yamada N. Thermodynamic analysis of expansion profile for displacement-type expander in low-temperature Rankine cycle. *J Therm Sci Technol* 2010;5:61–74. <https://doi.org/10.1299/jtst.5.61>. 1.
 - [12] Badr O, Probert SD, O'Callaghan P. Performances of multi-vane expanders. *Appl Energy* 1985;20:207–34.
 - [13] Mohd M, Tahir NY, Hoshino T. Efficiency of compact organic Rankine cycle system with rotary-vane-type expander for low-temperature waste heat recovery. *Int J Environ Sci Eng* 2010;2(1):11–6.
 - [14] Bao Junjiang, Zhao Li. A review of working fluid and expander selections for organic Rankine cycle. *Renew Sustain Energy Rev* 2013;24:325–42. <https://doi.org/10.1016/j.rser.2013.03.040>. ISSN 1364-0321.
 - [15] Imran Muhammad, Usman Muhammad, Park Byung-Sik, Lee Dong-Hyun. Volumetric expanders for low grade heat and waste heat recovery applications. *Renew Sustain Energy Rev* 2016;57:1090–109. <https://doi.org/10.1016/j.rser.2015.12.139>. ISSN 1364-0321.
 - [16] Vodicka V, Guillaume L, Mascuch J, Lemort V. Testing and modelling a vane expander used in an ORC working with hexamethyldioxane (MM) 3rd international seminar on ORC power systems. 2015. October 12–14.
 - [17] Ziviani Davide, Dickes Rémi, Lemort Vincent, James E, Braun, Groll Eckhard A. Effects of the working fluid charge in organic rankine cycle power systems: numerical and experimental analyses, organic rankine cycle technology for heat recovery. Rijeka: IntechOpen; 2018. <https://doi.org/10.5772/intechopen.78026>.
 - [18] Nordtvedt R. Experimental and theoretical study of a compression/absorption heat pump with ammonia/water as working fluid. 2005.
 - [19] Badr O, Probert SD, O'Callaghan P. Multi-vane expanders: internal-leakage losses. *Appl Energy* 1985;20(1):159–82.
 - [20] Badr O, O'Callaghan PW, Probert SD. Multi-vane expander performance: breathing characteristics. *Appl Energy* 1985;19(Issue 4):241–71. [https://doi.org/10.1016/0306-2619\(85\)90001-7](https://doi.org/10.1016/0306-2619(85)90001-7). ISSN 0306-2619.
 - [21] Vodicka Vaclav, Novotny Vaclav, Zeleny Zbynek, Mascuch Jakub, Kolovratnik Michal. Theoretical and experimental investigations on the radial and axial leakages within a rotary vane expander. *Energy* 2019;116097. <https://doi.org/10.1016/j.energy.2019.116097>. ISSN 0360-5442.
 - [22] Yang B, Peng X, He Z, Guo B, Xing Z. Experimental investigation on the internal working process of a CO2 rotary vane expander. *Appl Therm Eng* 2009;29(11–12):2289–96. <https://doi.org/10.1016/j.applthermaleng.2008.11.023>. ISSN 1359-4311.
 - [23] Jia Xiaohan, Zhang Bo, Pu Lei, Guo Bei, Peng Xueyuan. Improved rotary vane expander for trans-critical CO2 cycle by introducing high-pressure gas into the vane slots. *Int J Refrig* 2011;34(3):732–41. <https://doi.org/10.1016/j.ijrefrig.2010.12.005>. ISSN 0140-7007.
 - [24] Cipollone R. Sliding vane rotary compressor technology and energy saving. In: 8th international conference on compressors and their systems. Woodhead Publishing; 2013. ISBN 9781782421696. p. 27–54. <https://doi.org/10.1533/9781782421702.1.27>.
 - [25] Platts H. Hydrodynamic lubrication of sliding vanes. 187. In: *Proceedings of the international compressor engineering conference*. Purdue University; 1976. docs.lib.purdue.edu/icec/187/.
 - [26] Vodicka Vaclav, Novotny Vaclav, Mascuch Jakub, Kolovratnik Michal. Impact of major leakages on characteristics of a rotary vane expander for ORC. *Energy Procedia* 2017;129:387–94. <https://doi.org/10.1016/j.egypro.2017.09.249>. ISSN 1876-6102.
 - [27] Fatigati Fabio, Di Bartolomeo Marco, Di Battista Davide, Cipollone Roberto. Experimental and numerical characterization of the sliding rotary vane expander intake pressure in order to develop a novel control-diagnostic procedure. *Energies* 2019;12. <https://doi.org/10.3390/en12101970>. 10, 1970, 1996-1073.
 - [28] Kolasinski P, Biasiak P, Rak J. Experimental and numerical analyses on the rotary vane expander operating conditions in a micro organic rankine cycle system. *Energies* 2016;9(8):606. <https://doi.org/10.3390/en9080606>. <https://www.mdpi.com/1996-1073/9/8/606>.
 - [29] Bianchi Giuseppe, Rane Sham, Ahmed Kovacevic, Cipollone Roberto, Murgia Stefano, Contaldi Giulio. Numerical CFD simulations on a small-scale ORC expander using a customized grid generation methodology. *Energy Procedia* 2017;129:843–50. <https://doi.org/10.1016/j.egypro.2017.09.199>. ISSN 1876-6102.
 - [30] Mascuch Jakub, Novotny Vaclav, Vodicka Vaclav, Jan Spale, Zeleny Zbynek. Experimental development of a kilowatt-scale biomass fired micro – CHP unit based on ORC with rotary vane expander. *Renewable Energy*; 2018. <https://doi.org/10.1016/j.renene.2018.08.113>. ISSN 0960-1481.
 - [31] Fatigati Fabio, Bianchi Giuseppe, Cipollone Roberto. Development and numerical modelling of a supercharging technique for positive displacement expanders. *Applied Thermal Engineering*; 2018. <https://doi.org/10.1016/j.applthermaleng.2018.05.046>. ISSN 1359-4311.
 - [32] Fatigati Fabio, Di Bartolomeo Marco, Cipollone Roberto. Dual intake rotary vane expander technology: experimental and theoretical assessment. *Energy Convers Manag* 2019;186:156–67. <https://doi.org/10.1016/j.enconman.2019.02.026>. ISSN 0196-8904.
 - [33] Wang E, Zhang H, Fan B, Ouyang M, Zhao Y, Mu Q. Study of working fluid selection of organic rankine cycle (orc) for engine waste heat recovery. *Energy* 2011;36(5):3406–18. <https://doi.org/10.1016/j.energy.2011.03.041>.
 - [34] Macián V, Serrano JR, Dolz V, Sánchez J. Methodology to design a bottoming Rankine cycle, as a waste energy recovering system in vehicles. Study in a HDD engine. *Appl Energy* 2013;vol. 104:758–71. <https://doi.org/10.1016/j.apenergy.2012.11.075>. ISSN 0306-2619.
 - [35] Pili Roberto, Romagnoli Alessandro, Spliethoff Hartmut, Wieland Christoph. Economic feasibility of organic rankine cycles (ORC) in different transportation sectors. *Energy Procedia* 2017;105:1401–7. <https://doi.org/10.1016/j.egypro.2017.03.521>. ISSN 1876-6102.
 - [36] Gamma Technologies. GT Suite Flow Theory Manual. Version 2018. Chapter 1: Flow Solver Basics. Pages 1–12.
 - [37] Gamma Technologies. GT Suite Flow Theory Manual. Version 2018. Chapter 2: Flow Components and Connections. Pages 35–44.
 - [38] Gnutek Z, Kolasinski P. The application of rotary vane expanders in organic rankine cycle systems—thermodynamic description and experimental results. *May 20 ASME J Eng Gas Turbines Power* 2013;135(6):061901. <https://doi.org/10.1115/1.4023534>. June 2013.

Gli autori dichiarano di aver contribuito in misura paritetica allo sviluppo del presente articolo scientifico:
"On the effects of leakages in Sliding Rotary Vane Expanders", pubblicato sulla rivista internazionale
Energy, (<https://doi.org/10.1016/j.energy.2019.116721>).

Gli Autori:

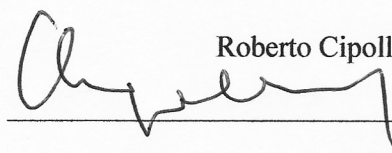
Fabio Fatigati

L'AQUILA, 24/09/2021 Fabio Fatigati

Marco Di Bartolomeo

L'AQUILA 24/09/2021 Marco Di Bartolomeo

Roberto Cipollone

 L'AQUILA 26/09/2021